Imaging Of Blood Flow Using Hyperpolarized ^{13}C-Urea In Preclinical Murine Models

C. von Morze[1], P. E. Larson[1], S. Hu[1], K. Keshari[1], D. M. Wilson[1], J. H. Ardenkjaer-Larsen[2], J. Kurhanewicz[1], and D. B. Vigneron[1]
[1]Department of Radiology and Biomedical Imaging, UCSF, San Francisco, CA, United States, [2]GE Healthcare, Hillerød, Denmark

Introduction: Tumors exhibit altered, heterogeneous patterns of blood flow due to abnormal neovascularization (1). Furthermore, changes in tumor blood flow during chemotherapy can predict pathologic response in locally advanced breast cancer (2). The use of metabolically inactive hyperpolarized molecules like urea for imaging of blood flow (3,4) has several advantages over the use of gadolinium(Gd)–containing compounds, including direct proportionality of signal to concentration, inherently high CNR, lower molecular weight, and the freedom to use safe endogenous substances. In this study, we demonstrate for the first time dynamic volumetric imaging of hyperpolarized [^{13}C]urea *in vivo* with 6 s time resolution, in five normal rats and five mice (three normal, two bearing transgenic liver tumors). For this project, we developed a new balanced SSFP pulse sequence with progressive flip angle excitations, for efficient imaging of hyperpolarized media. The blood flow measurements provide key physiological information, distinguishing well-perfused from poorly-perfused potentially hypoxic regions of tumor, which is complementary to the metabolic data from hyperpolarized [1-^{13}C]pyruvate MRSI. Furthermore, a perfusion-metabolism mismatch is thought to be an important prognostic variable in cancer (5). Therefore, we studied the combined results of bSSFP imaging of hyperpolarized [^{13}C]urea, and EPSI of [1-^{13}C]pyruvate and its metabolites, in mice. We also investigated the simultaneous co-polarization of pyruvate and urea to design a single MRSI experiment with information on both metabolism and perfusion, in five additional mice (one normal, four TRAMP transgenic prostate cancer mice). **Methods:** Urea samples were prepared by dissolving 99% [^{13}C]urea (Sigma-Aldrich, St. Louis, MO) in glycerol (6.4 M), with 15 mM GE trityl radical (GE Healthcare, Oslo, Norway). For each experiment, a sample was weighed and loaded into the Hypersense DNP polarizer (Oxford Instruments UK), where it was cooled to 1.4 K and irradiated by microwaves (94.095 GHz) in a magnetic field of 3.35 T for approximately one hour, and subsequently rapidly dissolved in a heated solution of phosphate buffered saline (1x PBS). The measured T1 was 47 s *ex vivo* (at 3T). Rats and mice were injected with a 2.4 mL and a 350 µL bolus, respectively, of urea solution (125mM) over twelve seconds, followed by a small saline flush. Animals were scanned on a GE 3T MR scanner, with dual-tuned ^{1}H / ^{13}C transmit-receive RF coils. Pulse sequence parameters: 2D multi-slice bSSFP with progressive flip angle over time, matrix= 32x32, FOV= 8cm, freq. direction= RL, pFOV=0.75, 8 slices x 8mm, TR=11.5ms, TE=5.75ms, spatial res = 2.5mm x 2.5mm x 8mm, imaging time = 2.2sec / stack. Initial and final θ/2 pulses were applied. Scanning commenced at the start of the injection, and the stack was repeated every 6 seconds, for a total of 6 repetitions over 30 seconds. The flip angles were selected based on a simulation of the hyperpolarized bSSFP signal, taken from (3), modified for dynamic acquisitions (T1=15sec, T2=300ms), selected to maintain proportionality of signal to the concentration of urea. An initial flip angle of θ=4° was empirically chosen. On the images, urea signal dynamics were quantified for the kidneys and the liver. Peak signals were measured, and blood flow maps were generated by matrix deconvolution of the blood flow from the tracer concentration-time curves. For comparison to the results from the urea, metabolic activity of the normal and tumor-bearing mice was studied by echo-planar spectroscopic imaging (EPSI) of hyperpolarized [1-^{13}C]pyruvate. The mice were injected with 350 µL 80mM [1-^{13}C]pyruvate in Tris buffer. At 30 s following intravenous administration of [1-^{13}C]pyruvate, high resolution 3D spectroscopic images (16x16x16, 2.5mm x 2.5mm x 5.4mm, spectral bandwidth=581 Hz, covering lactate to pyruvate at 3T) were acquired using previously described methods: EPSI with adiabatic double spin echo preparation (6), with 4-fold resolution enhancement using compressed sensing (7). Scan duration was 16 s. For the co-polarization experiments, samples of pyruvate and urea were measured as above and then loaded as frozen layers in the sample cup to prevent mixing, by quickly immersing the cup in a liquid nitrogen bath between each stage of loading. Imaging was by the EPSI sequence described above (with urea folding into the spectral region between lactate and alanine). Full sets of axial, sagittal, and coronal multi-slice T2-weighted FSE ^{1}H images were also acquired for all animals (192x192, FOV= 10 cm, 2mm slices, NEX=6). All hyperpolarized imaging data were registered to these anatomic scans, using custom software.

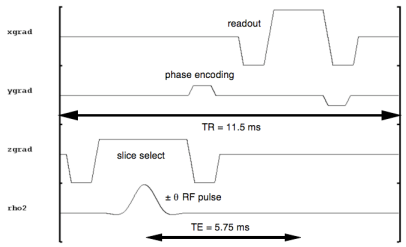

Fig. 1- bSSFP pulse sequence for dynamic imaging of hyperpolarized media

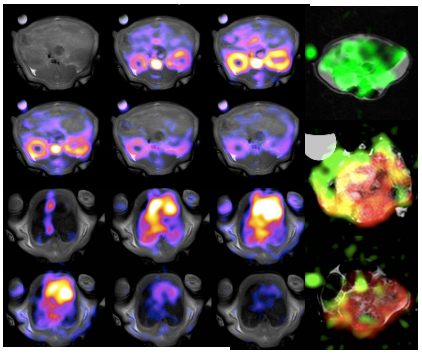

Fig. 2- Axial images of hyperpolarized [^{13}C]urea over 30 seconds in a normal rat, overlaid on ^{1}H T2-weighted FSE images. Top half- Kidneys and a portion of liver. Bottom half- Heart, descending aorta, and lungs.

Fig. 3- Hyperpolarized ^{13}C-urea (green) and ^{13}C-lactate (red), overlaid on T2-weighted FSE ^{1}H images (grayscale) of mouse liver, combining results of multiple experiments. Image 1- normal mouse. Images 2&3- liver tumor mice.

Results: In bSSFP imaging, rapid distribution of the urea to the heart and the kidneys was observed by the second time point (6 s), as well as diffuse pulmonary enhancement. The urea signal in the heart and kidneys peaked at 12 s. The right and left chambers of the rat heart were distinguishable. Diffuse enhancement of the liver was observed by the third or fourth time point (12 - 18 s). While there was substantial variation in blood flow data obtained between exams (as expected due to variation in physiology among animals, polarization levels achieved, delays prior to injection, etc.), the mean ratio of renal to hepatic blood flows among the rats was consistent with published "gold standard" results obtained using radioactive microspheres (8). The mean ratio of renal to hepatic blood flow obtained using our methods was 3.1, by region of interest analysis of the blood flow maps, while the "gold standard" ratio was 2.9. Differences in the patterns of blood flow to the liver were observed in tumor-bearing mice as compared to normal controls. While normal mouse liver exhibited a uniform, intermediate level of blood flow, the tumors were relatively poorly-perfused, with a few regions of high enhancement. These findings are consistent with published descriptions of blood flow in solid tumors (1). In combination with the results of MRSI of hyperpolarized [1-^{13}C]pyruvate, tumor regions with low urea signal and high lactate represented poorly perfused, hypoxic regions. These regions are shown in pure red in Figure 3, while well perfused regions of tumor are shown in yellow (green plus red). The same interpretation applies to the results of the co-polarization experiments shown in Fig. 4, which also shows regions of high and low perfusion within the prostate tumor.

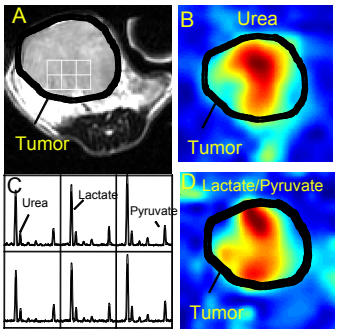

Fig. 4.- Results of co-polarization of urea & pyruvate in a transgenic model of prostate cancer. Heterogeneous perfusion is observed within tumor.

Discussion: Specialized hyperpolarized [^{13}C]urea MR techniques were developed and applied to obtain imaging measurements of relative blood flow in preclinical animal studies. In cancer models, the described methods provided the important added information on tissue perfusion to the metabolic information obtained using hyperpolarized [1-^{13}C]pyruvate.

Acknowledgements- We acknowledge grant funding from NIH EB007588 and GE A109773.

References- 1. Gillies et al. *Neoplasia*. 1999. 2. Dunnwald et al. *J Clin Oncol.* 2008. 3. Svensson et al. *MRM*. 2003. 4. Johansson et al. *MRM*. 2004. 5. Komar et al. *Clin Cancer Res.* 2009. 6. Cunningham et al. *JMR*. 2007. 7. Hu et al. *MRM*. 2008. 8. Tsuchiya et al. *Am Journ Physio*. 1978.